Conformationally Constrained Analogues of Diacylglycerol (DAG). 31. Modulation of the Biological Properties of Diacylgycerol Lactones (DAG-lactones) Containing Rigid-Rod Acyl Groups Separated from the Core Lactone by Spacer Units of Different Lengths

Maria J. Comin,[†] Gabriella Czifra,[‡] Noemi Kedei,[‡] Andrea Telek,[‡] Nancy E. Lewin,[‡] Sofiya Kolusheva,[§] Julia F. Velasquez,[‡] Ryan Kobylarz,[‡] Raz Jelinek,[§] Peter M. Blumberg,[‡] and Victor E. Marquez*[,†]

Laboratory of Medicinal Chemistry, Center for Cancer Research, National Cancer Institute—Frederick, National Institutes of Health, 376 Boyles Street, Frederick, Maryland 21702, Laboratory of Cancer Biology and Genetics, Center for Cancer Research, National Cancer Institute, National Institutes of Health, Bethesda, Maryland 20892, and Department of Chemistry and Ilse Katz Institute for Nanotechnology, Ben Gurion University, Beer Sheva 84105, Israel

Received February 13, 2009

Diacylglycerol lactones built with a rigid 4-[(methylphenyl)ethynyl]phenyl rod that is separated from the exocyclic acylcarbonyl of the DAG-lactone core by a spacer unit of variable length were synthesized and studied. Binding affinities for a panel of classical and novel PKC isozymes in two different phospholipid environments, one corresponding to the plasma membrane of cells, were determined. The kinetics and site of translocation for the PKC isozymes α and δ upon treatment with the compounds were also studied as well as the early response of ERK phosphorylation and the late response of induction of apoptosis in the human prostatic carcinoma cell line LNCaP. Finally, the compounds were evaluated in terms of their interaction with biomimetic lipid/polydiacetylene membranes by the associated chromatic response. The different spatial disposition of the rigid structural motif on the DAG-lactones contributes to differential activity.

Introduction

Occupancy of a wide range of G-protein-coupled receptors and receptor tyrosine kinases triggers the hydrolysis of phosphatidylinositol 4,5-bisphosphate (PIP_2 [a]), leading to the release of membrane-bound diacylglycerol (DAG).[1] DAG in turn interacts with the DAG recognition domains, termed C1 domains, on multiple families of signaling proteins, including isoforms of protein kinase C, the chimerins, RasGRP, PKD, MRCK, Unc13, and DAG kinase.[2] The activation of conventional (cPKCs α, βI, βII, γ) and novel (nPKCs δ, ε, η, θ) protein kinase C isoforms has been studied in great detail and involves both recruitment to membranes and allosteric activation by DAG.[3] Specific molecular interactions of DAG with the lipid environment into which it and the C1 domains insert influence both processes. The physical properties of the membranes and the interplay between the membranes and the alkyl chains of the DAG are thus of great importance. The combination of these interactions controls the localization of an isozyme to specific intracellular compartments and correspondingly controls which substrates are accessible.[4]

The effective use of a DAG-lactone template as a more potent DAG surrogate has been well documented in our laboratory.[5] In a recent study, we extended this concept to include a series of DAG-lactones containing rigid rods composed of ethynylene-substituted aromatic spacers [oligo-(*p*-phenyleneethynylene)] as acyl groups.[6] These compounds were designed to achieve various levels of membrane organization and penetration and were investigated for their ability to bind and translocate PKC α and δ isoforms to plasma and internal membranes. Some of the DAG-lactones were able to induce a substantially prolonged translocation state relative to the parent DAG-lactone containing an equivalent flexible acyl chain.[6] More recently, we studied the thermodynamic features of some new DAG-lactones with specific small groups attached to the terminus of a rigid 4-(phenylethynyl)benzoyl chain which affected both the self-assembly of the molecules and their interactions with phospholipids.[7] The results suggested that these DAG-lactones are predominantly incorporated within fluid phospholipid phases rather than in the condensed phases formed by cholesterol and that the size and charge of the phospholipid headgroups did not seem to affect the DAG-lactone interactions with lipids.[7]

Because different extents of membrane penetration and preference for membrane subdomains might yield different patterns of response in the ability of DAG-lactones to interact or translocate different GFP-tagged isozymes, we designed a series of DAG-lactones with a rigid 4-[(methylphenyl)ethynyl]phenyl rod (red) that is separated from the acylcarbonyl of the DAG-lactone core [2-(hydroxymethyl)-4-(methylethylidene)-5-oxo-2-2,3-dihydrofuryl]methyloxocarbonyl] (blue) by a $-O(CH_2)_n-$ spacer of 1, 2, or 3 methylene units (**1a**−**c**, Figure 1). We compared these three new targets with compound **2** without a spacer.

We evaluated the compounds in both in vitro and in cellular systems: (1) We determined their binding affinities for a panel of classical and novel PKC isozymes, assayed in two different phospholipid environments, either 100% phosphatidylserine or a lipid mixture corresponding to that of the plasma membrane of cells; (2) we compared the kinetics and site of translocation for the PKC isozymes α and δ upon treatment with the compounds; (3) we measured the potencies of the compounds for the early response of ERK phosphorylation and for the late response of induction of apoptosis in the human prostatic

* To whom correspondence should be addressed. Phone: 301-846-5954. Fax: 301-846-6033. E-mail: marquezv@dc37a.nci.nih.gov.
[†] National Cancer Institute—Frederick.
[‡] National Cancer Institute.
[§] Ben Gurion University.

[a] Abbreviations: PKC, protein kinase C; DAG, diacylglycerol; PKD, protein kinase D; RasGRP, Ras guanyl releasing protein; MRCK, mytonic dystrophy kinase-related Cdc42-binding kinase; Unc13, uncoordination gene 13 product; PIP_2, phosphatidylinositol 4,5-bisphosphate.

10.1021/jm900186m CCC: $40.75
Published on Web 04/20/2009

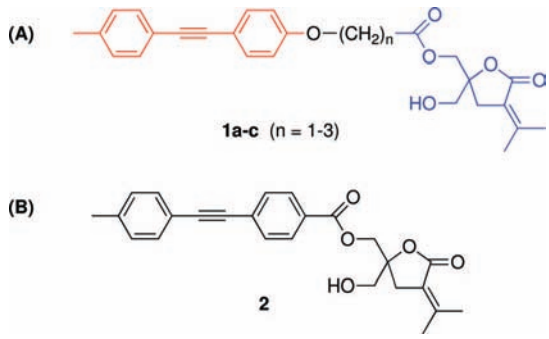

Figure 1. (A) ω-(4-[2-(Methylphenyl)ethynyl]phenoxy)alkanoyl DAG-lactones **1a**−**c**. The rigid rod moiety is indicated in red, the DAG-lactone in blue, and the variable linker in black. (B) [2-(Hydroxymethyl)-4-(methylethylidene)-5-oxo-2-2,3-dihydrofuryl]methyl, 4-[2-(4-methylphenyl)ethynyl]benzoate (compound **2**).

Scheme 1. Synthesis of *tert*-Butyl Esters

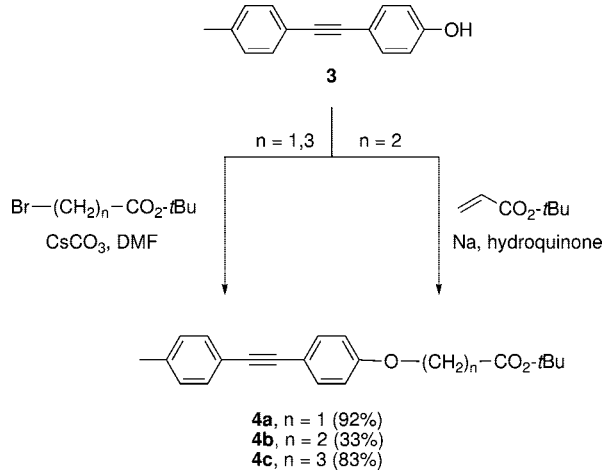

carcinoma cell line LNCaP; and (4) we evaluated the interaction of the compounds with a biomimetic lipid/polydiacetylene membrane by the associated chromatic response.

Results

Synthesis. Compound **2** was synthesized according to our previously published approach.[7] The preparation of racemic ω-(4-[2-(methylphenyl)ethynyl]phenoxy)alkanoyl monoesters of DAG-lactones (Figure 1) with one to three methylene spacers between the lactone and the rigid chain was achieved as depicted in Schemes 1 and 2. The rigid-rod component, 4-[2-(4-methylphenyl)ethynyl]phenol (**3**),[8] was prepared in excellent yield by a modified Sonogashira coupling between 4-iodophenol and 4-ethynyltoluene.[9] This phenol derivative was used as a building block for the preparation of all *tert*-butyl esters shown in Scheme 1. Thus, **4a** ($n = 1$) was obtained straightforwardly by treatment of **3** and *tert*-butyl 2-bromoacetate with cesium carbonate in excellent yield (92%).[10] Unfortunately, because of β-elimination, this was not the case when *tert*-butyl 3-bromopropanoate was used. Although the successful alkylation of phenols with β-propiolactone as the alkylating agent has been reported,[10] our reaction of **3** with β-propiolactone in the presence of *t*-BuOK or $CsCO_3$ led to mixtures of products. On the other hand, Michael addition of **3** to *tert*-butyl acrylate in the presence of catalytic amounts of sodium and hydroquinone[11] gave the desired *tert*-butyl ester **4b** ($n = 2$) in sufficient quantities to continue the synthesis. Despite the fact that several byproducts were obtained, including starting material **3**, the self-addition product of phenol to the triple bond, and cross-reaction between the starting phenol and desired product **4b**, successful separation of **4b** was achieved by simple column chromatography. The synthesis of the 3-methylene unit derivative was first attempted by reaction between **3** and γ-butyrolactone, but again, this method failed when applied to our system.[12] Starting from 4-bromobutanoic acid, the corresponding *tert*-butyl 4-bromobutanoate[13] was obtained in quantitative yield, and following nucleophilic displacement with **3** resulted in the desired 3-methylene unit, *tert*-butyl ester **4c**, in 83% yield (Scheme 1).

At this point, hydrolysis of *tert*-butyl esters was necessary to perform the acylation of the DAG-lactone moiety. Probably because of the presence of the triple bond, acidic hydrolysis of *tert*-butyl ester produced complex mixtures, even when triethylsilane was added as a carbocation scavenger.[14] However, thermolysis in quinoline at 205 °C [15] led cleanly to the desired free acids in quantitative yield which were isolated as crystalline solids (**5a**−**c**, Scheme 2). The use of bis(2-oxo-3-oxazolidinyl)phosphinic acid chloride (BOPCl) and dimethylaminopyridine (DMAP)[16] allowed the one-pot coupling of the acids with the free hydroxyl group of the monoprotected *O*-PMP-DAG-lactone **6**[6] (for $n = 1$ and 3) and *O*-benzyl-DAG-lactone **7**[6] (for $n = 2$) in very good yield. Removal of the *p*-methoxyphenyl (PMP) protecting group in the presence of ceric ammonium nitrate (CAN) to give the target compounds **1a** and **1c** resulted in low yields (54% and 50%) due to the presence of the additional phenoxy ether linkage in **8a** and **8c**. A better strategy was the coupling of the *O*-benzyl protected DAG-lactone **7** that led to the desired DAG-lactone **1b** in a markedly better yield (80%) after treatment with boron trichloride at low temperature (Scheme 2).

Biological Activity. Binding Affinity for PKC Isozymes. Enzyme−ligand interactions were assessed in vitro in terms of the ability of the ligand to displace bound [20-^{3}H]phorbol 12,13-dibutyrate (PDBu) from the recombinant human PKC isozymes in the presence of phosphatidylserine.[17] The partition coefficients (log *P*) were calculated according to the atom-based program MOE SlogP[18] (Table 1).

Each of the PKC isozymes showed a similar pattern of dependence on the length of the spacer for compounds **1a**−**c** (Table 1). In each case, the affinities increased (lower K_i) with the distance of the rigid rod from the DAG-lactone core, with compound **1c** ($n = 3$) being the most potent. In sharp contrast, however, the most potent of all ligands (**2**) lacks a spacer between these two units, suggesting a qualitatively different interaction between it, the enzymes, and the lipid environment. In terms of isozyme specificity, PKCε stood out from the other isoforms in showing a 5- to 4-fold lower affinity for compounds **1a** and **1b** with the shorter spacers. The other isozymes responded within similar ranges of concentration for each individual compound.

The above assays were carried out under standard conditions in which the PKC isoforms were assayed in the presence of 100 μg/mL phosphatidylserine, which provides a highly anionic surface. These conditions maximize the interaction of the PKC isoforms with the phospholipid bilayer. To detect differences in interactions that might depend on a more physiological lipid composition, we also assayed the isoforms in the presence of 100 μg/mL of a mixture of phosphatidylcholine/phosphatidylethanolamine/phosphatidylserine/phosphatidylinositol/cholesterol (12:35:22:9:21), a plasma membrane lipid (PML) mixture designed to mimic that of the inner leaflet of the plasma membrane.[19] We observed (Table 2, Figure 2) that the rigid rod compounds were generally several-fold less potent for the

Scheme 2. Synthesis of DAG-lactones

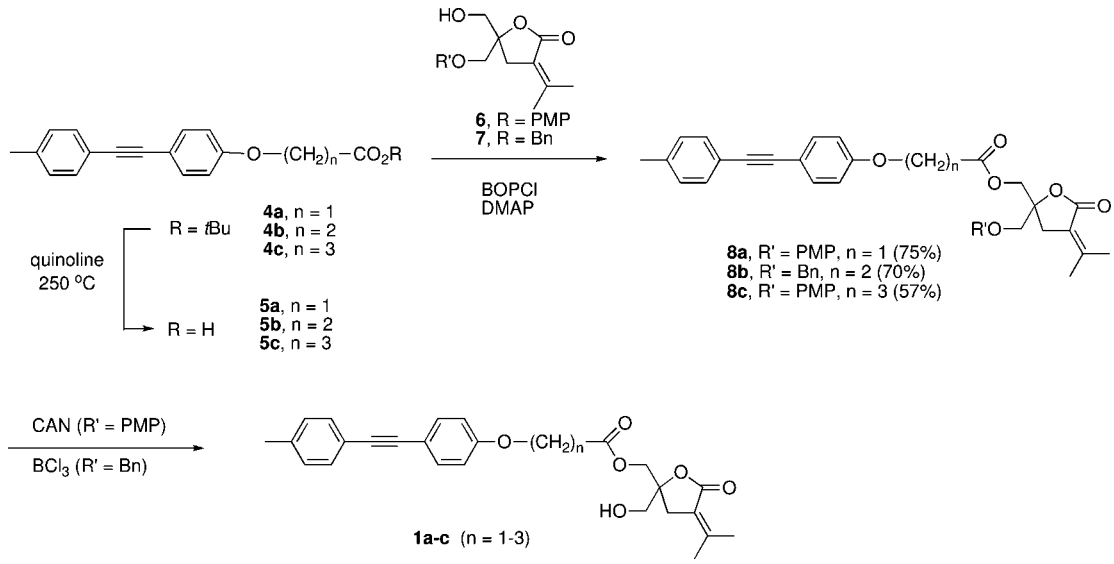

Table 1. Binding Affinities (K_i, nM) for PKC Isozymes (Average of Three Determinations ± SEM)

isozyme	**1a** ($n = 1$), log $P = 3.31$	**1b** ($n = 2$), log $P = 3.72$	**1c** ($n = 3$), log $P = 4.11$	**2**, log $P = 3.56$
PKCα	38 ± 14	20.8 ± 5.2	19.5 ± 0.74	6.0 ± 1.5
PKCβ	76 ± 15	57 ± 13	15.2 ± 3.1	4.1 ± 1.1
PKCγ	50.8 ± 6.0	35.0 ± 4.1	12.3 ± 1.2	6.2 ± 1.6
PKCδ	46.4 ± 3.6	35.8 ± 6.1	11.9 ± 0.4	5.4 ± 0.8
PKCε	268 ± 72	153 ± 12	37.9 ± 4.4	10.0 ± 1.2

Table 2. Binding Affinities (K_i, nM) for PKC Isozymes (Average of Three Determinations ± SEM) Assayed in the Presence of Plasma Membrane Lipid Mimetic Mixture

isozyme	**1a** ($n = 1$), log $P = 3.31$	**1b** ($n = 2$), log $P = 3.72$	**1c** ($n = 3$), log $P = 4.11$	**2**, log $P = 3.56$
PKCα	165.1 ± 2.8	143 ± 37	76 ± 15	15.8 ± 2.7
PKCβ	100.3 ± 6.9	66 ± 21	43.8 ± 4.7	12.6 ± 0.72
PKCγ	139.6 ± 3.7	78.0 ± 4.5	31.7 ± 2.8	15.7 ± 2.1
PKCδ	47.7 ± 6.1	31.3 ± 0.82	11.6 ± 2.3	2.74 ± 0.43
PKCε	147 ± 16	78.7 ± 9.1	31.9 ± 1.3	8.3 ± 1.5

classic PKC isoforms in the plasma membrane mimetic membranes as compared to the 100 μg/mL phosphatidylserine, whereas for the novel PKC isoforms they were equal or more potent.

ERK Phosphorylation in LNCaP Cells. Activation of the ERK pathway, as reflected by ERK phosphorylation, is a prominent early biological response to PKC stimulation by DAG-lactones and phorbol ester.[6] Because of the rapidity of the response, phosphorylation of ERK is relatively independent of issues of compound stability, so it provides a convenient measure of overall biological potency. All of the compounds caused phosphorylation of ERK in the concentration range of 1−10 μM (Figure 3). Similar to the potencies in the binding assays, increasing potency was observed as the length of the spacer was increased, with compounds **1b** and **1c** being the most potent. Likewise, compound **2**, which lacked any spacer, was the most potent of all four rigid rod compounds examined.

Apoptotic Activity. In the human prostatic carcinoma cell line LNCaP, apoptosis is induced both by phorbol esters and by DAG-lactones.[20] This response, which we measure at 2 days after treatment, lies downstream of several PKC isoforms, in particular PKCα and PKCδ, and will be influenced by the stability of the compounds as well as by their potencies and selectivities. As seen in Figure 4, all the compounds induced apoptosis, with an apparent preference for the longer spacers of **1b** and **1c**. It is noteworthy that compound **1c** induced a

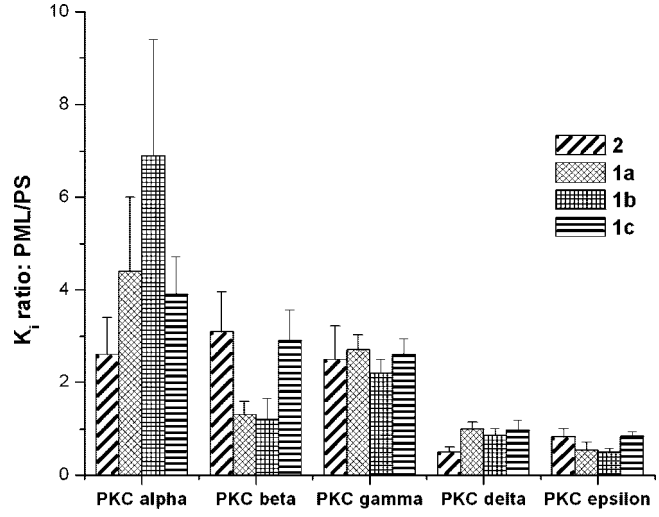

Figure 2. Effect of the lipid environment on the potencies of the rigid rod compounds for PKC isoforms. Compounds were assayed with the various PKC isoforms in the presence of either phosphatidylserine (PS) or a lipid mixture corresponding to the composition of the inner leaflet of the plasma membrane, as described in the methods section. Values represent the ratio of the K_i value with the plasma membrane lipid (PML) mimetic mixture to that with phosphatidylserine, where the K_i values are the average of three independent experiments. Error bars represent ±SEM.

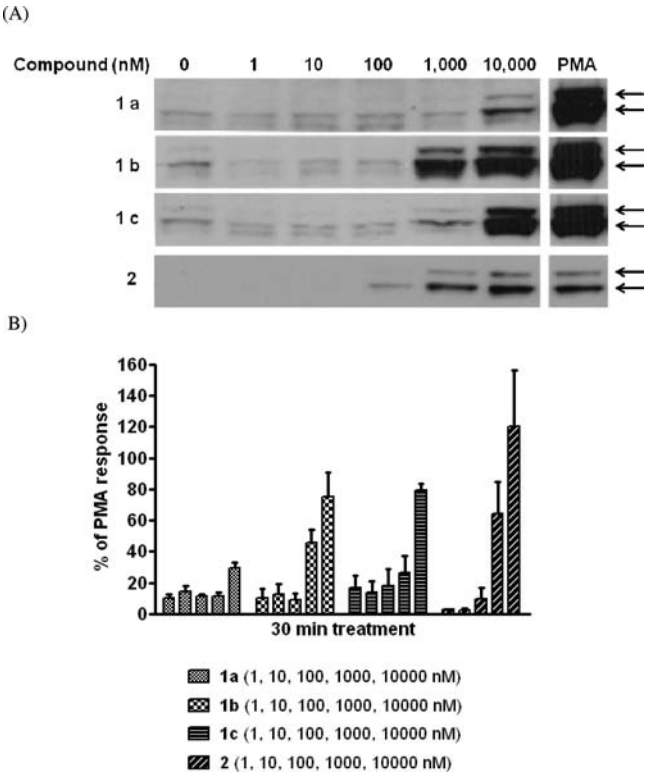

Figure 3. ERK phosphorylation induced by compounds **1a**−**c** and **2** in LNCaP cells. Cells were treated with the indicated compounds at the indicated nanomolar concentrations or with PMA (100 nM) for 30 min, and then ERK phosphorylation was determined by Western blotting. (A) Representative Western blot showing the phosphorylated p42/44 bands indicated by arrows (two additional independent experiments gave similar results). Control blots (data not shown) confirmed that the amounts of ERK did not change as a function of the ligand concentration. (B) Intensities of the bands of phosphorylated ERK were determined by densitometry. Bars represent the mean values from the three independent experiments. Error bars indicate the SEM.

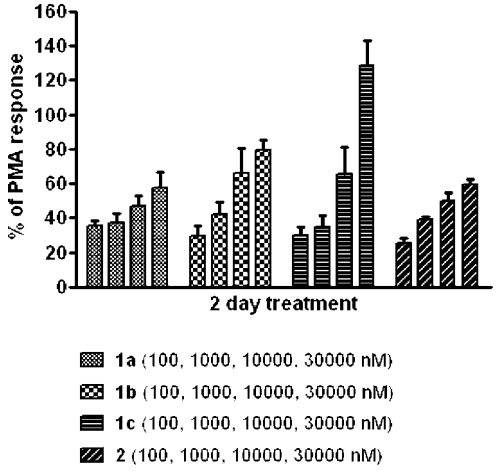

Figure 4. Dose−response of compounds **1a**−**c** and **2** for induction of apoptosis in LNCaP cells relative to 1000 nM PMA. Data are the mean ± SEM of three experiments (2 days of treatment).

higher level of apoptosis than did compound **2**, contrasting with the higher potency of **2** in the in vitro binding assays (Table 1).

Cellular Translocation of GFP-Tagged PKC Isoforms in CHO Cells. The above biological assays do not distinguish between PKC isoforms. Translocation of individual PKC isoforms from cytosol to membrane compartments provides a measure of their activation, can reveal differences in the kinetics of response, and may uncover differences in the distribution of an isoform between various membrane compartments.[21] We examined the pattern of response of PKCα (Figure 5) and PKCδ (Figure 6) as representatives of the classic and novel PKC isoforms, using green fluorescent protein fusion constructs heterologously expressed in Chinese hamster ovary cells. Results are summarized in Table 3.

For all derivatives, PKCα translocated to the plasma membrane, which is the typical response for this isoform. Compound **2** was the fastest acting compound on PKCα. As the length of the linker increased in the series **1a**−**c** the response became more rapid, although the response to **1c** remained slower than that to **2**. PKCδ shows a more variable pattern of response to various ligands, with PMA inducing initial translocation to the plasma membrane followed by redistribution to internal membranes and hydrophilic derivatives inducing the initial translocation to the internal membranes (not shown). Compound **2** translocated PKCδ mainly to the plasma membrane and nuclear membrane, but it was not PMA-like for PKCδ; there was no sequential translocation to the plasma membrane followed by a shift to nuclear membrane. Compounds **1a**−**c** translocated PKCδ mainly to the internal membranes, but it was noteworthy that localization was predominantly perinuclear rather than to the nuclear membrane per se.

Interactions of DAG-lactones with Artificial Membranes. Interactions of DAG-lactones with membranes are expected to cause perturbations that affect the structural and dynamic properties of the phospholipid bilayers. Visualization of these interactions is possible with the use of membranes that contain polydiacetylene (PDA) patches that are easily perturbed.[22,23] The PDA-based vesicle assay reports on the occurrence of membrane interactions through color and fluorescence transformations of the vesicle-embedded PDA patches induced through interactions of membrane-associated molecules with the vesicle bilayers.[24]

Figure 7 depicts the dose-dependent fluorescence chromatic response (% FCR) curves induced by the DAG-lactones following addition to biomimetic dimyristoylphosphatidylcholine (DMPC)/PDA vesicles. All four compounds gave rise to increasing fluorescence signals upon higher concentrations, indicating that the molecules exhibited membrane interactions. However, differences were apparent among the compounds with regards to the *extent* of induced chromatic response (intensity of fluorescence signal) and particularly the *shape* of the dose−response curves. Specifically, Figure 7 shows that **1a**, **1b**, and **1c** exhibited a relatively steep initial increase in % FCR with a subsequent moderate rise of the dose−response curve [or a slight *decrease* in % FCR in the case of **1a** (Figure 7, curve i), most likely due to severe precipitation]. Compound **2**, on the other hand, induced a very low chromatic response up to approximately 2 mM, followed by a pronounced increase in fluorescence emission, which subsequently exceeded the % FCS values induced by the three other molecules (Figure 7, iv).

Previous studies have shown that the features of the chromatic lipid/PDA dose−response curves are intimately affected by the mechanisms of membrane binding and insertion.[25] Accordingly, the pronounced difference between the fluorescence curve induced by **2** and the curves of **1a**−**c** indicates that DAG-lactone **2** exhibits a distinct lipid binding profile. In particular, the apparent parabolic shape of the chromatic response curve of **2** suggests that a self-assembly process precedes membrane binding and that this self-association might be a precondition for bilayer interactions.[26,27] Compounds **1a**−**c**, on the other hand, most likely undergo a simple concentration-dependent

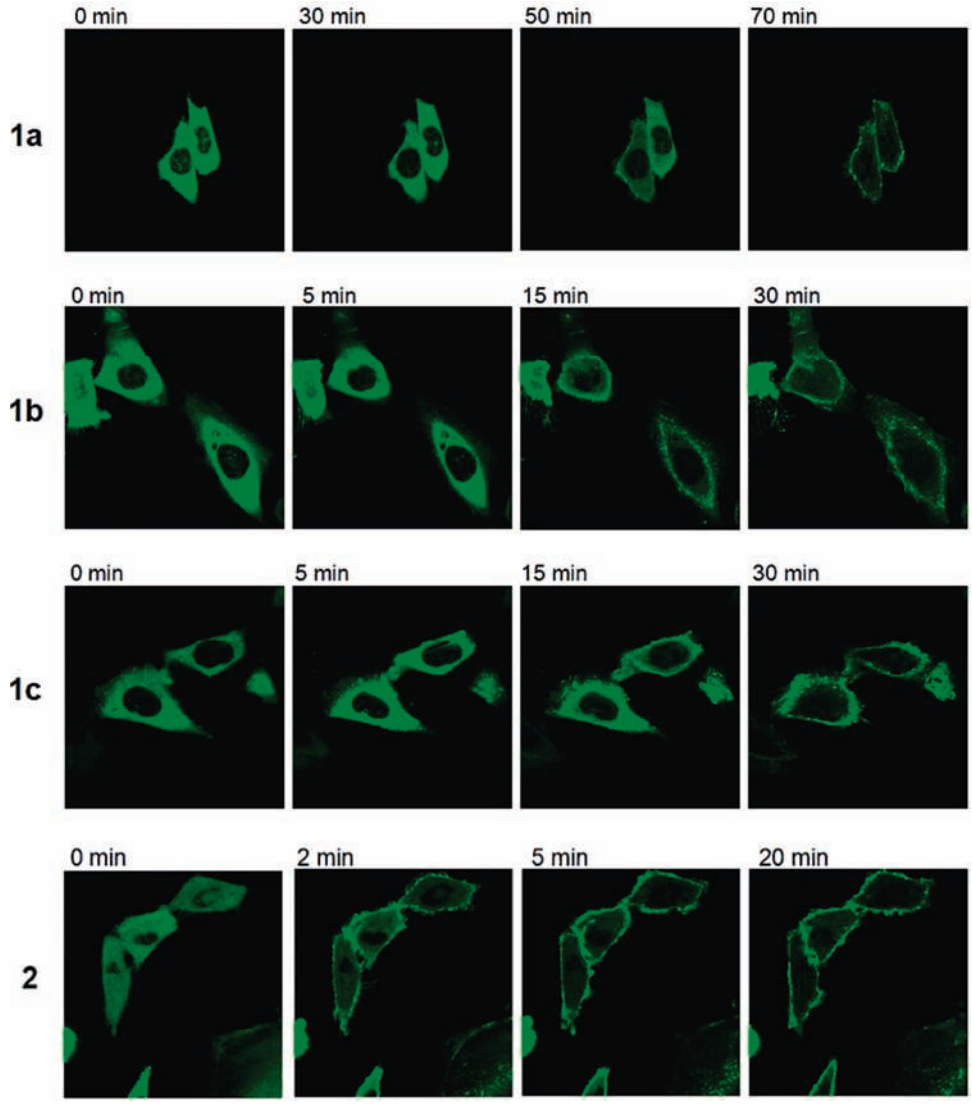

Figure 5. Translocation of GFP-PKCα in CHO cells in response to addition of DAG-lactones (10 μM). Cells expressing the GFP-PKCα were treated with 10 μM of the compounds. The redistribution of the fluorescent proteins was monitored with a Zeiss MRC 1024 confocal microscope as a function of time after the addition of the compounds. Images were captured every 30 s. Each panel represents a typical example from four independent experiments.

bilayer binding, as reflected in the dose−response curves in Figure 7 (i−iii).

Discussion

Protein kinase C has attracted great interest as a therapeutic target for cancer and other conditions in consequence of its central role in cellular signal transduction, mediating responses to the second messenger DAG.[28,29] Current PKC targeted drugs in clinical trials reflect two complementary strategies. Enzastaurin, an orally active PKC inhibitor that is relatively selective for PKCβ among the PKC isoforms, is directed at the catalytic site.[30] Like most kinase inhibitors, it faces the imposing challenge of distinguishing among the 500 plus kinases of the mammalian kinome, and it indeed shows off-target activity on several other kinases. Bryostatin 1[31] and PEP005,[32] on the other hand, are natural products, which interact with the DAG-phorbol ester responsive C1 domains shared by PKC, RasGRP, and the chimerins.

Although the mechanistic rationale for the therapeutic activity of C1 directed agents is less clear than for catalytic site directed agents, interest is driven by the demonstrated ability of different ligands for PKC to induce different biological responses, by the ability of bryostatin to antagonize many responses induced by phorbol esters, and by the demonstration that one PKC isoform may have effects antagonistic of another.[28] Opportunities for antagonism are further enhanced by the additional classes of C1 domain containing targets. For example, DAG kinases will terminate DAG signaling, and the chimerins, by inhibiting Rac, would be expected to be tumor suppressors.[2] In contrast to kinase inhibitors, a great opportunity for design of selectivity for C1 domain ligands is provided by the nature of the ligand interaction site, where not only the C1 domain but also the lipid environment with which it is associated contributes to ligand recognition.[4] Thus, for example, we have described very different selectivity for PMA relative to bryostatin between the PKCα and PKCδ isoforms in mouse 3T3 cells and mouse keratinocytes.[33,34] Likewise, using several libraries of DAG-lactones differing only in their patterns of side chains, modulating their lipid interactions, we have shown that different compounds were selective for different biological end points.[4] We describe here our initial characterization of a small series of compounds in which we have manipulated the length and

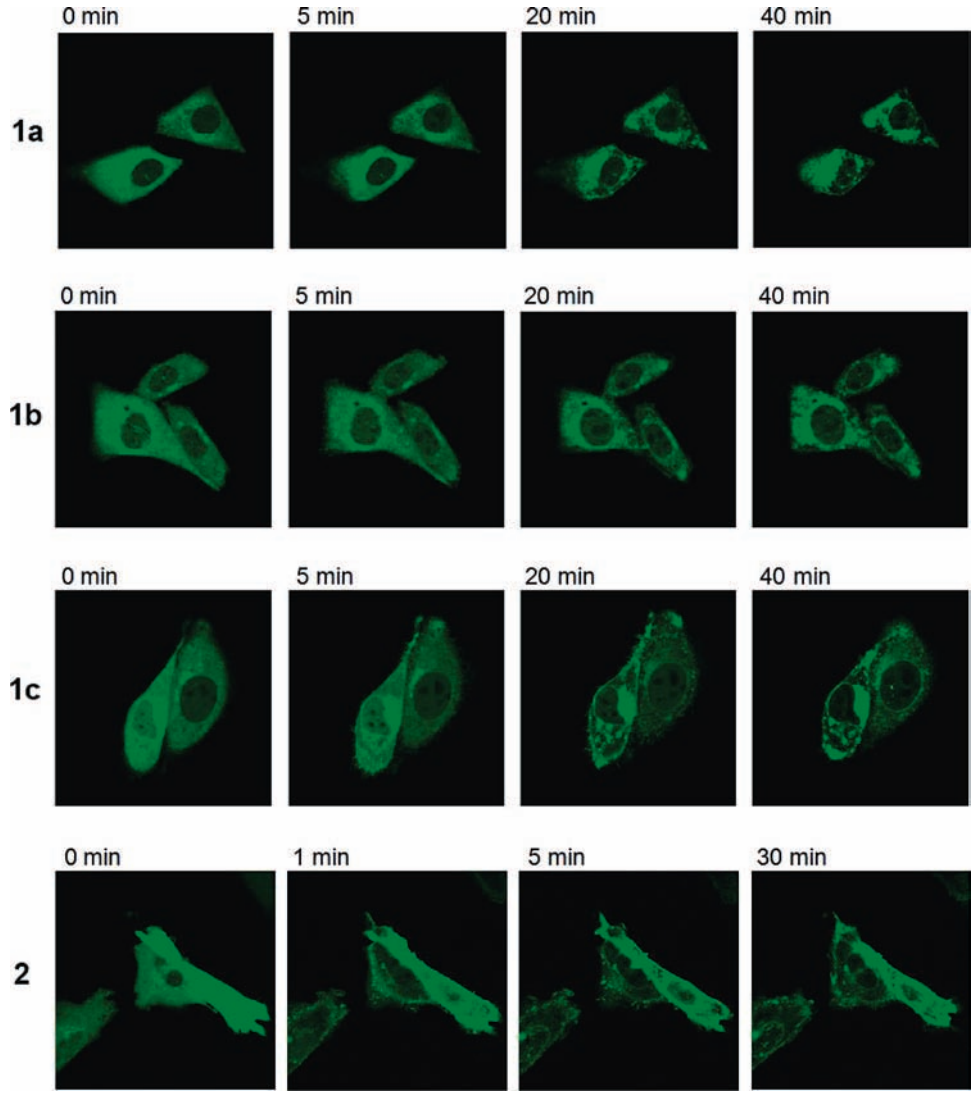

Figure 6. Translocation of GFP-PKCδ in CHO cells upon addition of DAG-lactones (10 μM). Cells expressing GFP-PKCδ were treated with 10 μM of the compounds as indicated. The redistribution of the fluorescent proteins was monitored with a Zeiss MRC 1024 confocal microscope as a function of time after the addition of the drugs. Images were captured every 30 s. Each panel represents a typical example from three independent experiments.

Table 3. Pattern of Translocation for PKCα and PKCδ in Response to DAG-lactones[a]

compd	kinetics of translocation of GFP-PKCα, plasma membrane	relative distribution of GFP-PKCδ		
		plasma membrane	nuclear membrane	internal membranes
1a	slowest	++	++	+++
1b	intermediate	+	+	+++
1c	intermediate	++	++	++
2	fast	+++	+++	+

[a] Intensities of localization are represented by the number of "+" marks. Results from three independent experiments are summarized.

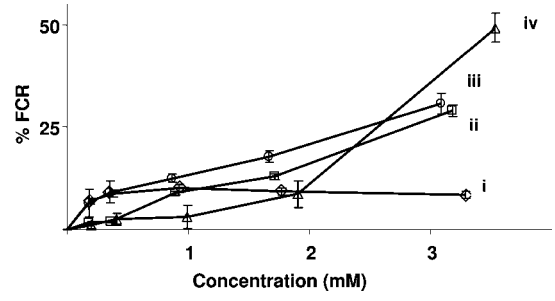

Figure 7. Chromatic dose−response curves. Fluorescence chromatic response (% FCR) induced by the DAG-lactones in DMPC/PDA vesicles: (i) **1a**; (ii) **1b**; (iii) **1c**; (iv) **2**.

nature of the connection of the DAG-lactone template and a rigid rod terminus on one side chain. We have previously observed that incorporation of a rigid rod structure into the side chain caused exclusion of the ligand from cholesterol rich subdomains, suggesting that such rigid structural motifs might contribute to differential recognition.[7] Lipid rafts rich in cholesterol are proposed to represent specialized areas for signaling complexes in the plasma membrane,[35] and plasma membranes differ from those of internal membranes such as the nuclear membrane in being overall richer in cholesterol.[36]

Other types of specialized lipid subdomains have also been described.[37] Here, we observed that the rigid rod compounds were relatively less active on the classic PKC isoforms in membranes containing cholesterol and relatively deficient in phosphatidylserine compared to those constituted solely of phosphatidylserine. We also observed that the potencies of the compounds in vitro depended not only on the log *P* but also on the particular nature of the linker, emphasizing the importance

of the specific interactions with the lipid. At the biological level, we noted differences in induction of the downstream response of ERK phosphorylation by the various compounds, as we did for apoptotic response and PKC isoform translocation.

The biomimetic lipid/PDA vesicle assay showed that DAG-lactones exhibited significant membrane interactions; however, there appears to be a pronounced difference between the *mechanism* of membrane association between DAG-lactone **2** and the other three compounds with variable tethers. Specifically, the chromatic dose−response analysis in Figure 6 might suggest that **2** undergoes a distinct self-assembly process (possibly forming micelles or similar aggregates) prior to membrane binding; the consequent aggregates are therefore the likely entities exhibiting affinity to the membrane bilayer rather than the individual molecules.

More extensive exploration of the influence of the positioning of rigid rod substituents on the recognition of DAG lactones and clarification of the linkage between mechanistic differences and biological consequences should be of considerable interest.

Experimental Section

Analysis of Inhibition of [^{3}H]PDBu Binding by Nonradioactive Ligands. Enzyme−ligand interactions were analyzed by competition with [^{3}H]PDBu binding to a single isozyme essentially as described previously.[17] As indicated in the text, the PKC isozymes were assayed in the presence of 100 μg/mL phosphatidylserine or else 100 μg/mL total lipid, where the lipid composition was chosen to mimic that of the inner leaflet of the plasma membrane. This latter composition was phosphatidylcholine/phosphatidylethanolamine/phosphatidylserine/phosphatidylinositol/cholesterol (12:35:22:9:21). The ID_{50} values were determined by least-squares fitting of the theoretical sigmoidal competition curve to the binding data. The K_i values were calculated from the ID_{50} values according to the relationship $K_i = ID_{50}/(1 + L/K_d)$, where L is the concentration of free [^{3}H]PDBu at the ID_{50} and K_d is the dissociation constant for [^{3}H]PDBu under the assay conditions. Values represent the mean ± standard error of the mean for three independent experiments. The octanol/water partition coefficients (log P) were calculated according to the atom-based program MOE SlogP.[18]

[^{3}H]PDBu was from PerkinElmer (Waltham, MA). 1-Palmitoyl-2-oleoylphosphatidylcholine, 1-palmitoyl-2-oleoylphosphatidylethanolamine, 1-palmitoyl-2-oleoylphosphatidylserine, and bovine liver phosphatidylinositol were from Avanti Polar Lipids (Alabaster, AL). Cholesterol was from Sigma (St. Louis, MO). The human PKCα, PKCβ, PKCγ, PKC δ, and PKCε were from Invitrogen (Carlsbad, CA).

ERK Phosphorylation in LNCaP Cells. Androgen-sensitive LNCaP prostate cancer cells were purchased from the American Type Culture Collection (Manassas, VA) and cultured in RPMI-1640 medium supplemented with 10% fetal bovine serum and antibiotics (penicillin at 50 units/mL and streptomycin at 0.05 mg/mL). Cells were plated in 6 cm dishes at about 60% confluency and 24 h later were treated with different concentrations of the test compound and 100 nM PMA for 30 min. After treatment, the cells were washed with phosphate buffered saline, total cell lysates were prepared, and the lysates were analyzed by 10% SDS−PAGE followed by electrotransfer and immunostaining. The primary antibodies used for immunostaining against phospho-ERK (9101) and total ERK (9102) were from Cell Signaling (Danvers, MA). The immunostaining was visualized by ECL (Amersham Biosciences). Films were scanned, and densitometry was performed using Image J (developed at National Institute of Mental Health, NIH).

Apoptosis in LNCaP Cells. LNCaP cells plated in 10 cm dishes at about 60% confluency were treated with different concentrations of the test compound and of 1 μM PMA for 48 h. After treatment, the cells were washed and resuspended in phosphate buffered saline. YO-PRO-1 (Invitrogen, Carlsbad, CA) was added to a final concentration of 1 μM, and the cells were incubated for 20 min at 4 °C in the dark. 7-Aminoactinomycin D (7-AAD) (Invitrogen, Carlsbad, CA) was then added at a 5 μg/mL final concentration 10 min before analysis by flow cytometry using the FACSCalibur system (Becton Dickinson, Mountain View, CA). Data were analyzed with FlowJo 7 (Tree Star, Inc. Ashland, OR). The Yo-Pro-1 positive cells were considered apoptotic and were expressed as % of total cells.

Translocation of GFP-Tagged PKC Isoforms in CHO Cells. CHO cells were purchased from the American Type Culture Collection (Manassas, VA) and cultured in F12-K medium supplemented with 10% fetal bovine serum and antibiotics (penicillin at 50 units/mL and streptomycin at 0.05 mg/mL). CHO cells plated onto T delta dishes (Bioptechs Inc., Butler, PA) were transfected with GFP-tagged PKCα or PKCδ using Lipofectamine reagent (Invitrogen, Carlsbad, CA). Cells were visualized with a Zeiss LSM 510 confocal microscope (Carl Zeiss Inc., Thornwood, NY) with an Axiovert 100M inverted microscope operating with a 25 mW argon laser tuned to 488 nm. Cells were imaged with a 63 × 1.4 NA Zeiss Plan Apochromat oil immersion objective and with varying zooms (1.4−2). Time-lapse images were collected every 30 s using the Zeiss AIM software, in which the green emission was collected in a PMT with a LP 505 filter.

Vesicle Preparation. Vesicle emulsions containing DMPC and TRCDA (2:3 molar ratio) were prepared as previously described.[25] Briefly, the lipid constituents were dried together in vacuo followed by addition of deionized water and sonication at 70 °C. The vesicle emulsion was then cooled to room temperature and kept at 4 °C overnight; it was then polymerized by irradiation at 254 nm for 30 s. The resulting emulsion exhibits a blue appearance. Vesicle samples for experiments were prepared at concentrations of 0.5 mM (total lipids) in 50 mM Tris-Cl, pH 8. The various compounds at different concentrations were mixed with the vesicles prior to addition of the Tris buffer. All compounds were dissolved in DMSO (10 mg/mL).

Multiwell Fluorescence Spectroscopy. Samples were prepared by adding different volumes of the compounds in DMSO solutions to 30 μL of the dimyristoylphosphatidylcholine (DMPC) and diacetylene 10,12-tricosadiynoic acid (TRCDA) vesicles, followed by addition of 30 μL of 50 mM Tris base buffer (pH 8). Samples were placed in Greiner 96-microwell plates. Fluorescence intensity was measured using a multiwell fluorescence plate reader (Fluoroscan Ascent; Thermo, Finland) with a 485/555 nm excitation/emission long path filter set. The fluorescence percentage was calculated as percentage intensity compared to the fully transformed red vesicles. All measurements were carried out at 27 °C.

Synthetic Methods. General. All chemical reagents were commercially available. Melting points were taken on a Fisher-Jones apparatus and are uncorrected. Combi-flash column chromatography was performed on silica gel 60 (230−240 mesh) employing a Teledyne Isco instrument, and analytical TLC was performed on Analtech Uniplates silica gel GF. Unless otherwise indicated, NMR spectra were determined in $CDCl_3$ (99.8%) with residual $CHCl_3$ as the reference peak (7.26 and 77.0 ppm) and were recorded on a Varian 400 MHz spectrophotometer. The coupling constants are reported in hertz, and the peak shifts are reported in the δ (ppm) scale; abbreviations used are s (singlet), d (doublet), dd (doublet-of-doublets), ddd (doublet-of-doublet-of-doublets), t (triplet), q (quartet), and m (multiplet). Positive-ion fast-bombardment mass spectra (FABMS) were obtained on a VG 7070E mass spectrometer at an accelerating voltage of 6 kV and a resolution of 2000. Glycerol was used as the sample matrix, and ionization was effected by a beam of xenon atoms. Combustion analyses were performed for all intermediates and final products to confirm that their level of purity was ≥95%; they were performed by Atlantic Microlab. Inc., Norcross, GA. Infrared spectroscopy data were obtained neat with a Jasco FT-IR/615 spectrometer. Specific optical rotations were measured in a Perkin-Elmer model 241 polarimeter. All reaction glassware was oven-dried and cooled to room temperature in an argon atmosphere prior to use.

4-[2-(4-Methylphenyl)ethynyl]phenol (3). 4-Ethynyltoluene (5.0 g, 43.04 mmol) was added to a solution of 4-iodophenol (9.2 g, 41.79 mmol), $Pd(PPh_3)_2Cl_2$ (590 mg, 0.84 mmol), CuI (320 mg, 1.67 mmol), and Et_3N (8.5 mL, 60.9 mmol) in THF (50 mL) at room temperature under an argon atmosphere. The reaction mixture was stirred overnight. The solids were separated by filtration, and the volatiles were evaporated under reduced pressure. The residue was purified by combi-flash column chromatography (silica gel; hexanes/ethyl acetate, 4:1) to give 8.3 g (95% yield) of pure **3** as a yellowish solid: mp 124 °C (lit.[7] 103−104 °C); FTIR (neat) 3307 cm^{-1}; ^1H NMR (400 MHz, $CDCl_3$) δ 7.42 (m, 4 H, Ph), 7.14 (dm, $J = 7.8$ Hz, 2 H, Ph), 6.80 (dm, $J = 8.8$ Hz, 2 H, Ph), 4.80 (bs, 1 H, −*OH*), 2.36 (s, 3 H, −C*H*$_3$); ^{13}C NMR (100 MHz, $CDCl_3$) δ 155.45, 138.07, 133.20, 133.14, 131.35, 131.29, 129.08, 120.37, 115.45, 88.49, 88.19, 21.43. FABMS *m*/*z* (relative intensity): 209 (MH^+, 36), 208 ($M^{+\bullet}$, 100). Anal. Calcd for $C_{14}H_{10}O \cdot 0.2H_2O$: C, 85.06; H, 5.30. Found: C, 84.98; H, 5.59.

4-Methyl-1-[(phenyl)ethyny]benzene, *tert*-Butyl 2-hydroxyacetate (4a). *tert*-Butyl bromoacetate (0.85 mL, 5.58 mmol) was added to a suspension of **3** (1.02 g, 4.90 mmol) and $CsCO_3$ (2.55 g, 7.76 mmol) in anhydrous DMF (12 mL) at room temperature under argon. The reaction mixture was stirred for 5 h. Et_2O (50 mL) was added, and the solution was washed with $NaHCO_3$ (2 × 15 mL) and water (1 × 15 mL) before it was dried ($MgSO_4$) and concentrated. The residue was purified by combi-flash column chromatography (silica gel; hexanes/EtOAc, 9:1) to give 1.43 g (92% yield) of pure **4a** as a yellowish solid: mp 85 °C, FTIR (neat) 1751 cm^{-1}; ^1H NMR (400 MHz, $CDCl_3$) δ 7.45 (dm, $J = 8.9$ Hz, 2 H, Ph), 7.40 (dm, $J = 8.1$ Hz, 2 H, Ph), 7.14 (dm, $J = 8.1$ Hz, 2 H, Ph), 6.86 (dm, $J = 8.9$ Hz, 2 H, Ph), 4.52 (s, 2 H, H-2), 2.36 (s, 3 H, −C*H*$_3$), 1.48 (s, 9 H, −C(C*H*$_3$)$_3$); ^{13}C NMR (100 MHz, $CDCl_3$) δ 167.69, 157.74, 138.07, 132.95, 131.33, 129.05, 120.37, 116.52, 114.60, 88.44, 88.40, 82.52, 65.65, 28.01, 21.47. FABMS *m*/*z* (relative intensity): 323 (MH^+, 44), 322 ($M^{+\bullet}$, 100). Anal. Calcd for $C_{21}H_{22}O_3$: C, 78.23; H, 6.88. Found: C, 78.29; H, 6.91.

(2-[(4-Methoxyphenoxy)methyl]-4-(methylethylidene)-5-oxo-2-2,3-dihydrofuryl)methyl 2-(4-[2-(4-Methylphenyl)ethynyl]phenoxy)acetate (8a). A solution of *tert*-butyl ester **4a** (1.34 g, 0.42 mmol) in quinoline (30 mL) was heated to 205 °C for 3 h. The mixture was cooled to room temperature and was poured into 1.2 M HCl (30 mL) at 0 °C. The solid free acid was filtered, washed with 1.2 M HCl and water, and dried under vacuum overnight at 100 °C. A solution of **6** (151 mg, 0.52 mmol) in CH_2Cl_2 (5 mL) was added to a suspension of free acid **5a** (151 mg, 0.57 mml) in CH_2Cl_2 (10 mL). DMAP (158 mg, 1.29 mmol) and BOPCl (263 mg, 1.38 mmol) were successively added, and the reaction mixture was stirred for 1 h at room temperature under argon. NH_4Cl (ss, 10 mL) was added, and the mixture was extracted with CH_2Cl_2 (3 × 20 mL). The combined organic phases were washed with brine (2 × 10 mL), dried ($MgSO_4$), and concentrated. The residue was purified by combi-flash column chromatography (hexanes/EtOAc, 4:1) to give a 210 mg (75%) of **8a** as a foam: FTIR (neat) 1748 cm^{-1}; ^1H NMR (400 MHz, $CDCl_3$) δ 7.41 (m, 4 H, Ph), 7.15 (dm, $J = 7.9$ Hz, 2 H, Ph), 6.76−6.84 (m, 6 H, Ph), 4.68 (s, 2 H, H-2), 4.68 (s, 2 H, −C*H*$_2$OCOCH$_2$OAr), 3.95 (d, $J = 9.5$ Hz, 1 H, −C*H*$_a$HOPMP), 3.84 (d, $J = 9.5$ Hz, 1 H, −CH*H*$_b$OPMP), 3.74 (s, 3 H, −OC*H*$_3$), 2.89 (dm, $J = 16.7$ Hz,1 H, H-3$_a$), 2.64 (dm, $J = 16.7$ Hz,1 H, H-3$_b$), 2.36 (s, 3 H, −C*H*$_3$), 2.27 (br s, 3 H, −C*H*$_3$), 1.86 (s, 3 H, −C*H*$_3$); ^{13}C NMR (100 MHz, $CDCl_3$) δ 168.39, 168.27, 157.40, 154.46, 152.34, 152.13, 138.16, 132.96, 133.04, 131.21, 129.07, 120.27, 118.02, 116.87, 115.57, 114.68, 114.46, 88.67, 88.24, 79.10, 69.99, 66.23, 64.91, 55.65, 32.67, 24.60, 21.45, 19.99. FABMS *m*/*z* (relative intensity): 541 (MH^+, 78), 540 ($M^{+\bullet}$, 100). Anal. Calcd for $C_{33}H_{32}O_7 \cdot 0.8H_2O$: C, 71.46; H, 6.11. Found: C, 71.33; H, 5.86.

[2-(Hydroxymethyl)-4-(methylethylidene)-5-oxo-2-2,3-dihydrofuryl]methyl 2-(4-[2-(4-Methylphenyl)ethynyl]phenoxy)acetate (1a). Cerium ammonium nitrate (CAN, 247 mg, 0.45 mmol) was added to a solution of **8a** (81 mg, 0.15 mmol) in acetonitrile/water (4:1, 5 mL) at 0 °C. After 10 min, 5% $Na_2S_2O_3$ solution (10 mL) was added and the mixture was extracted with EtOAc (3 × 20 mL). The organic phase was washed with brine (10 mL), dried ($MgSO_4$), and concentrated. The residue was purified by combi-flash column chromatography (silica gel; hexanes/EtOAc, 1:1) to give 35 mg (54% yield) of pure **1a** as a white solid: mp 147 °C. FTIR (neat) 3447, 1746 cm^{-1}; ^1H NMR (400 MHz, $CDCl_3$−CD_3OD) δ 7.30 (dm, $J = 8.9$ Hz, 2 H, Ph), 7.24 (dm, $J = 8.2$ Hz, 2 H, Ph), 7.00 (dm, $J = 8.2$ Hz, 2 H, Ph), 6.71 (dm, $J = 8.9$ Hz, 2 H, Ph), 4.55 (s, 2 H, H-2), 4.18 (ABq, $J = 11.7$ Hz, 2 H, −C*H*$_2$OCOCH$_2$OAr), 3.44 (mAB, 2 H, −C*H*$_2$OH), 2.59 (dm, $J = 16.5$ Hz, 1 H, H-3a), 2.42 (dm, $J = 16.5$ Hz,1 H, H-3b), 2.21 (s, 3 H, −C*H*$_3$), 2.09 (br s, 3 H, −C*H*$_3$), 1.70 (s, 3 H, −C*H*$_3$); ^{13}C NMR (100 MHz, $CDCl_3$) δ 169.54, 168.47, 157.23, 152.19, 138.02, 132.77, 131.05, 128.84, 119.97, 118.50, 116.65, 114.29, 88.40, 87.93, 81.14, 65.88, 64.68, 64.11, 31.56, 24.23, 21.08, 19.63. FABMS *m*/*z* (relative intensity): 435 (MH^+, 99), 434 ($M^{+\bullet}$, 100). Anal. Calcd for $C_{26}H_{26}O_6 \cdot 0.3H_2O$: C, 71.04; H, 6.10. Found: C, 71.06; H, 6.07.

***tert*-Butyl 3-(4-[2-(4-Methylphenyl)ethynyl]phenoxy)propanoate (4b).** A solution of **3** (1.05 g, 5.04 mmol) in *tert*-butyl acrylate (5 mL) was treated with sodium (3.5 mg, cat.) and hydroquinone (1 mg, cat.). The mixture was stirred at room temperature for 2 h. Et_2O (20 mL) and a drop of acetic acid were added, and the solution was washed with water (2 × 10 mL), dried ($MgSO_4$), and concentrated. The residue was purified by combi-flash column chromatography (silica gel; hexanes/EtOAc, 9:1) to give 550 mg (33% yield) of pure **4b** as a yellowish solid: mp 74 °C. FTIR (neat) 1731 cm^{-1}; ^1H NMR (400 MHz, $CDCl_3$) δ 7.42 (m, 4 H, Ph), 7.14 (dm, $J = 7.8$ Hz, 2 H, Ph), 6.87 (dm, $J = 8.9$ Hz, 2 H, Ph), 4.23 (t, $J = 6.5$ Hz, 2 H, H-3), 2.71 (t, $J = 6.5$ Hz, 2 H, H-2), 2.36 (s, 3 H, −C*H*$_3$), 1.47 (s, 9 H, −C(C*H*$_3$)$_3$); ^{13}C NMR (100 MHz, $CDCl_3$) δ 170.06, 158.51, 137.91, 132.87, 131.26, 129.00, 120.42, 115.75, 114.55, 88.59, 88.19, 80.92, 63.72, 35.62, 28.02, 21.40. FABMS *m*/*z* (relative intensity): 337 (MH^+, 41), 336 ($M^{+\bullet}$, 100). Anal. Calcd for $C_{22}H_{24}O_3$: C, 78.24; H, 7.19. Found: C, 78.48; H, 7.21.

(4-(Methylethylidene)-5-oxo-2-[(phenylmethoxy)methyl]-2-2,3-dihydrofuryl)methyl 3-(4-[2-(4-Methylphenyl)ethynyl]phenoxy)propanoate (8b). *tert*-Butyl ester **4b** was treated in the same way as that described for **4a** and the corresponding free acid was reacted with **7** as described for the synthesis of **8a** to give 180 mg (70% yield) of **8b** as a colorless oil. FTIR (neat) 1744 cm^{-1}; ^1H NMR (400 MHz, $CDCl_3$) δ 7.42−7.25 (m, 9 H, Ph), 7.11 (dm, $J = 7.9$ Hz, 2 H, Ph), 6.80 (dm, $J = 8.9$ Hz, 2 H, Ph), 4.50 (s, 2 H, −OC*H*$_2$Ph), 4.25 (s, 2 H, −C*H*$_2$OCOCH$_2$CH$_2$OAr), 4.18 (t, $J = 6.3$ Hz, 2 H, H-3), 3.49 (ABq, $J = 9.9$ Hz, 2 H, −C*H*$_2$OBn), 2.77 (t, $J = 6.3$ Hz, 2 H, H-2), 2.78 (dm, $J = 16.4$ Hz, 1 H, H-3$_a$), 2.62 (dm, $J = 16.4$ Hz,1 H, H-3$_b$), 2.33 (s, 3 H, −C*H*$_3$), 2.20 (t, $J = 2.0$ Hz, 3 H, −C*H*$_3$), 1.76 (s, 3 H, −C*H*$_3$); ^{13}C NMR (100 MHz, $CDCl_3$) δ 170.26, 168.83, 158.25, 151.28, 138.05, 137.44, 132.96, 131.31, 129.05, 128.43, 127.86, 127.64, 120.39, 118.74, 116.07, 114.51, 88.48, 79.94, 73.65, 71.72, 66.19, 63.20, 34.40, 32.72, 24.47, 21.47, 19.89. FABMS *m*/*z* (relative intensity): 539 (MH^+, 31), 538 ($M^{+\bullet}$, 35). Anal. Calcd for $C_{34}H_{34}O_6 \cdot 0.6H_2O$: C, 74.38; H, 6.46. Found: C, 74.05; H, 6.16.

[2-(Hydroxymethyl)-4-(methylethylidene)-5-oxo-2-2,3-dihydrofuryl]methyl 3-(4-[2-(4-Methylphenyl)ethynyl]phenoxy)propanoate (1b). A solution of **8b** (141 mg, 0.26 mmol) in anhydrous CH_2Cl_2 (5 mL) was treated with 1.0 M BCl_3 solution in CH_2Cl_2 (1 mL, 1.05 mmol) at −78 °C for 15 min. $NaHCO_3$ (ss, 5 mL) was added, and the mixture was allowed to reach room temperature. The aqueous layer was extracted with CH_2Cl_2 (3 × 20 mL), and the combined organic layers were dried ($MgSO_4$) and concentrated. The residue was purified by combi-flash column chromatography (silica gel; hexanes/EtOAc, 1:1) to give 93 mg (80% yield) of pure **1b** as a white solid: mp 125 °C. FTIR (neat) 3472, 1731 cm^{-1}; ^1H NMR (400 MHz, $CDCl_3$) δ 7.45−7.38 (m, 4 H, Ph), 7.14 (dm, $J = 8.0$ Hz, 2 H, Ph), 6.84 (dm, $J = 8.9$ Hz, 2 H, Ph), 4.28 (ABq, $J = 11.8$ Hz, 2 H, −C*H*$_2$OCOCH$_2$CH$_2$OAr), 4.23 (t, $J = 6.3$ Hz, 2 H, H-3), 3.66 (ABq, $J = 12.1$ Hz, 2 H, −C*H*$_2$OH), 2.83 (t, $J = 6.3$ Hz, 2 H, H-2), 2.78 (dm, $J = 16.5$ Hz, 1 H, H-3$_a$), 2.64 (dm, $J = 16.4$ Hz,1 H, H-3$_b$), 2.35 (s, 3 H, −C*H*$_3$), 2.23 (t, $J = 2.0$ Hz, 3 H, −C*H*$_3$), 1.80 (s, 3 H, −C*H*$_3$); ^{13}C NMR (100 MHz, $CDCl_3$)

δ 170.66, 168.91, 158.18, 152.14, 138.06, 132.98, 131.30, 129.05, 120.34, 118.59, 116.14, 114.49, 88.43, 88.39, 80393, 65.66, 64.82, 63.22, 34.42, 32.01, 24.53, 21.45, 19.96; FABMS *m/z* (relative intensity): 449 (MH^+, 85), 448 ($M^{+\bullet}$, 100). Anal. Calcd for $C_{27}H_{28}O_6 \cdot 0.3H_2O$: C, 71.49; H, 6.35. Found: C, 71.30; H, 6.18.

***tert*-Butyl 4-(4-[2-(4-Methylphenyl)ethynyl]phenoxy)butanoate (4c).** This compound was prepared similarly as described for **4a** from *tert*-butyl 4-bromobutanoate (302 mg, 2.43 mmol) and phenol **3** (253 mg, 2.21 mmol). After combi-flash column chromatography (silica gel; hexanes/ethyl acetate, 9:1) 351 mg (83% yield) of pure **4c** was obtained as a yellowish solid: mp 68 °C. FTIR (neat) 1723 cm^{-1}; ^1H NMR (400 MHz, $CDCl_3$) δ 7.45 (dm, $J = 8.3$ Hz, 2 H, Ph), 7.40 (dm, $J = 7.8$ Hz, 2 H, Ph), 7.14 (dm, $J = 7.8$ Hz, 2 H, Ph), 6.85 (dm, $J = 8.3$ Hz, 2 H, Ph), 4.01 (t, $J = 6.2$ Hz, 1 H, H-4), 2.43 (t, $J = 7.3$ Hz, 1 H, H-2), 2.36 (s, 3 H, $-CH_3$), 2.07 (m, 2 H, H-3), 1.45 (s, 9 H, $-C(CH_3)_3$); ^{13}C NMR (100 MHz, $CDCl_3$) δ 172.39, 158.78, 137.92, 132.90, 131.27, 129.02, 120.47, 115.52, 114.45, 88.65, 88.14, 80.34, 31.91, 28.07, 24.66, 21.43; FABMS *m/z* (relative intensity): 351 (MH^+, 16), 350 ($M^{+\bullet}$, 41). Anal. Calcd for $C_{23}H_{26}O_3 \cdot 0.1H_2O$: C, 78.48; H, 7.50. Found: C, 78.32; H, 7.47.

(2-[(4-Methoxyphenoxy)methyl]-4-(methylethylidene)-5-oxo-2-2,3-dihydrofuryl)methyl 4-(4-[2-(4-Methylphenyl)ethynyl]phenoxy)butanoate (8c). *tert*-Butyl ester **4c** (342 mg, 0.98 mmol) was treated in the same manner as described for **4a**, and the corresponding free acid was reacted with **6** (202 mg, 0.69 mmol) as described for the synthesis of **8a** to give 224 mg (57% yield) of **8c** as a white solid: mp 117 °C; FTIR (neat) 1744 cm^{-1}; ^1H NMR (400 MHz, $CDCl_3$) δ 7.44−7.39 (m, 4 H, Ph), 7.14 (dm, $J = 7.9$ Hz, 2 H, Ph), 6.82 (m, 6 H, Ph), 4.34 (ABq, $J = 11.8$ Hz, 2 H, $-CH_2OCOCH_2CH_2CH_2OAr$), 3.99 (t, $J = 6.0$ Hz, 2 H, H-4), 3.98 (ABq, $J = 9.5$ Hz, 2 H, $-CH_2OPMP$), 3.76 (s, 3 H, $-OCH_3$), 2.96 (dm, $J = 16.4$ Hz, 1 H, H-3_a), 2.75 (dm, $J = 16.4$ Hz, 1 H, H-3_b), 2.55 (t, $J = 7.3$ Hz, 2 H, H-2), 2.36 (s, 3 H, $-CH_3$), 2.28 (br s, 3 H, $-CH_3$), 2.09 (m, 2 H, H-3), 1.87 (s, 3 H, $-CH_3$); ^{13}C NMR (100 MHz, $CDCl_3$) δ 172.55, 168.63, 158.61, 154.43, 152.28, 151.82, 138.00, 132.96, 131.30, 129.05, 120.45, 118.44, 115.61, 114.68, 114.44, 88.60, 88.23, 79.41, 70.22, 66.52, 65.88, 55.69, 32.88, 30.53, 24.60, 24.45, 21.47, 19.97. FABMS *m/z* (relative intensity): 569 (MH^+, 100), 568 ($M^{+\bullet}$, 86). Anal. Calcd for $C_{35}H_{36}O_7 \cdot 0.4H_2O$: C, 73.05; H, 6.45. Found: C, 72.85; H, 6.38.

[2-(Hydroxymethyl)-4-(methylethylidene)-5-oxo-2-2,3-dihydrofuryl]methyl 4-(4-[2-(4-Methylphenyl)ethynyl]phenoxy)butanoate (1c). Starting from **8c**, compound **1c** was obtained as described for **1a** in 50% yield: mp 115−116 °; FTIR (neat) 3428, 1714 cm^{-1}; ^1H NMR (400 MHz, $CDCl_3$) δ 7.44−7.38 (m, 4 H, Ph), 7.13 (dm, $J = 7.8$ Hz, 2 H, Ph), 6.84 (dm, $J = 8.9$ Hz, 2 H, Ph), 4.23 (ABq, $J = 11.8$ Hz, 2 H, $-CH_2OCOCH_2CH_2CH_2OAr$), 4.00 (t, $J = 6.0$ Hz, 2 H, H-4), 3.65 (m, 2 H, $-CH_2OH$), 2.80 (dm, $J = 16.5$ Hz, 1 H, H-3_a), 2.62 (dm, $J = 16.5$ Hz, 1 H, H-3_b), 2.56 (t, $J = 7.3$ Hz, 2 H, H-2), 2.35 (s, 3 H, $-CH_3$), 2.25 (br s, 3 H, $-CH_3$), 2.10 (m, 2 H, H-3), 1.85 (s, 3 H, $-CH_3$); ^{13}C NMR (100 MHz, $CDCl_3$) δ 172.91, 168.90, 158.57, 151.94, 138.01, 132.95, 131.29, 129.04, 120.41, 118.70, 115.75, 114.43, 88.55, 88.25, 80.97, 66.54, 65.52, 64.80, 32.09, 30.55, 24.57, 24.43, 21.45, 19.96; FABMS *m/z* (relative intensity): 463 (MH^+, 100), 462 ($M^{+\bullet}$, 84). Anal. Calcd for $C_{28}H_{30}O_6 \cdot 0.4H_2O$: C, 71.64; H, 6.61. Found: C, 71.58; H, 6.41.

[2-(Hydroxymethyl)-4-(methylethylidene)-5-oxo-2-2,3-dihydrofuryl]methyl 4-[2-(4-Methylphenyl)ethynyl]benzoate (2). This compound was prepared by the same methodology as described in ref 7. Pure **2** (260 mg, 76%) was obtained as a yellowish solid: mp 167−168 °C; FTIR (neat) 3469, 2214, 1723 cm^{-1}; ^1H NMR (400 MHz, $CDCl_3$) δ 7.96 (m, 2 H, Ph), 7.57 (m, 2 H, Ph), 7.44 (m, 2 H, Ph), 7.18 (m, 2 H, Ph), 4.58 (mAB, 2 H, $-Ph\text{-}CO_2CH_2-$), 3.76 (ABq, $J = 12.1$ Hz, 2 H, $HOCH_2-$), 2.90−2.70 (m*AB*, 2 H, H-$4_{a,b}$), 2.38 (s, 3 H, $-CH_3$), 2.25 (t, $J = 2.0$ Hz, 3 H, $-CH_3$), 1.86 (s, 3 H, $-CH_3$); ^{13}C NMR (100 MHz, $CDCl_3$) δ 169.10, 165.78, 151.67, 139.09, 131.62, 131.46, 129.61, 129.18, 128.82, 128.23, 119.00, 93.12, 87.88, 81.45, 66.32, 64.78, 32.25, 24.55, 21.53, 19.91. FABMS *m/z* (relative intensity): 405 (MH^+, 47). Anal. Calcd for $C_{25}H_{24}O_5 \cdot 0.3H_2O$: C, 73.26; H, 6.05. Found: C, 73.21; H, 5.99.

Acknowledgment. This research was supported in part by the Intramural Research Program of the NIH, National Cancer Institute, Center for Cancer Research. We also thank Drs. James A. Kelley and Chris Lai for HRMS measurements and Dr. Dina M. Sigano for help with the calculations of log *P* values and assembling the manuscript.

Supporting Information Available: ^1H and ^{13}C spectra for **1a**−**c**. This material is available free of charge via the Internet at http://pubs.acs.org.

References

(1) Rhee, S. G. Regulation of phosphoinositide-specific phospholipase C. *Annu. Rev. Biochem.* **2001**, *70*, 281–312.

(2) Griner, E. M.; Kazanietz, M. G. Protein kinase C and other diacylglycerol effectors in cancer. *Nat. Rev Cancer* **2007**, *7*, 281–294.

(3) For a recent review, see the following: Steinberg, S. F. Structural basis of protein kinase C isoform function. *Physiol. Rev.* **2008**, *88*, 1341–1378.

(4) Duan, D.; Sigano, D. M.; Kelley, J. A.; Lai, C.; Lewin, N. E.; Kedei, N.; Peach, M. L.; Lee, J.; Abeyweera, T. P.; Rotenberg, S. A.; Kim, H.; Kim, Y. H.; El Kazzouli, S.; Chung, J.-U.; Young, H. A.; Young, M.; Baker, A.; Colburn, N. H.; Haimovitz-Friedman, A.; Truman, J.-P.; Parrish, D. A.; Deschamps, J. R.; Perry, N. A.; Surawski, R. J.; Blumberg, P. M.; Marquez, V. E. Conformationally constrained analogues of diacylglycerol (DAG). 29. Cells sort DAG-lactone chemical zip codes to produce diverse and selective biological activities. *J. Med. Chem.* **2008**, *51*, 5198–5220.

(5) Marquez, V. E.; Blumberg, P. M. Synthetic diacylglycerols (DAG) and DAG-lactones as activators of protein kinase C (PK-C). *Acc. Chem. Res.* **2003**, *36*, 434–443.

(6) Malolanarasimhan, K.; Kedei, N.; Sigano, D. M.; Kelley, J. A.; Lai, C. C.; Lewin, N. E.; Surawski, R. J.; Pavlyukovets, V. A.; Garfield, S. H.; Wincovitch, S.; Blumberg, P. M.; Marquez, V. E. Conformationally constrained analogues of diacylglycerol (DAG). 27. Modulation of membrane translocation of protein kinase C (PKC) isozymes alpha and delta by diacylglycerol lactones (DAG-lactones) containing rigid-rod acyl groups. *J. Med. Chem.* **2007**, *50*, 962–978.

(7) Philosof-Mazor, L.; Volinsky, R.; Comin, M. J.; Lewin, N. E.; Kedei, N.; Blumberg, P. M.; Marquez, V. E.; Jelinek, R. Self-assembly and lipid interactions of diacylglycerol lactone derivatives studied at the air/water interface. *Langmuir* **2008**, *24*, 11043–11052.

(8) Veschamb, H.; Dauphin, G.; Kergomar, A. Transmission of electronic effects in molecules of trans 4-hydroxystilbenes and 4-hydroxy tolanes. *Bull. Soc. Chim. Fr.* **1967**, *8*, 2846–2854.

(9) Thorand, S.; Krause, N. J. Improved procedures for the palladium-catalyzed coupling of terminal alkynes with aryl bromides (Sonogashira coupling). *J. Org. Chem.* **1998**, *63*, 8551–8553.

(10) Hajduk, P. J.; Sheppard, G.; Nettesheim, D. G.; Olejniczak, E. T.; Shuker, S. B.; Meadows, R. P.; Steinman, D. H.; Carrera, G. M.; Marcotte, P. A.; Severin, J.; Walter, K.; Smith, H. E.; Simmer, R.; Holzman, T. F.; Morgan, D. W.; Davidsen, S. K.; Summers, J. B.; Fesik, S. W. Discovery of potent nonpeptide inhibitors of stromelysin using SAR by NMR. *J. Am. Chem. Soc.* **1997**, *119*, 5818–5827.

(11) Schmidt, U.; Lieberknecht, A.; Griesser, H.; Talbiersky, J. Synthesis of peptide alkaloids. 5. New method for synthesis of ansa peptides. Amino acids and peptides. 34. *J. Org. Chem.* **1982**, *47*, 3261–3264.

(12) Rueeger, H.; Gerspacher, M.; Buehlmayer, P.; Rigollier, P.; Yamaguchi, Y.; Schmidlin, T.; Whitebread, S.; Nuesslein-Hildesheim, B.; Nick, H.; Cricione, L. Discovery and SAR of potent, orally available and brain-penetrable 5,6-dihydro-4*H*-3-thia-1-aza-benzo[*e*]azulen- and 4,5-dihydro-6-oxa-3-thia-1-aza-benzo[*e*]azulen derivatives as neuropeptide YY5 receptor antagonists. *Bioorg. Med. Chem. Lett.* **2004**, *14*, 2451–2457.

(13) Patel, M.; Goswami, A.; Chu, L.; Donovan, M. J.; Nanduri, V.; Goldberg, S.; Johnston, R.; Siva, P. J.; Nielsen, B.; Fan, J. Y.; He, W. X.; Shi, Z. P.; Wang, K. W.; Eiring, R.; Cazzulino, D.; Singh, A.; Mueller, R. Enantioselective microbial reduction of substituted acetophenones. *Tetrahedron: Asymmetry* **2004**, *15*, 1247–1258.

(14) Mehta, A.; Jaouhari, R.; Benson, T. J.; Douglas, K. T. Improved efficiency and selectivity in peptide synthesis: use of triethylsilane as a carbocation scavenger in deprotection of t-butyl esters and t-butoxycarbonyl-protected sites. *Tetrahedron Lett.* **1992**, *33*, 5441–5444.

(15) Lampe, J. W.; Hughes, P. F.; Biggers, C. K.; Smith, S. H.; Hu, H. Total synthesis of (−)- and (+)-balanol. *J. Org. Chem.* **1996**, *61*, 4572–4581.

(16) Diago-Meseguer, J.; Palomo-Coll, A.; Fernandez-Lizarbe, J. R.; Zugaza-Bilbao, A. A new reagent for activating carboxyl groups; preparation and reactions of *N,N*-bis[2-oxo-3-ox-azolidinyl]phosphorodiamidic chloride. *Synthesis* **1980**, *54*, 7–551.

(17) Lewin, N. E.; Blumberg, P. M. [^{3}H]Phorbol 12,13-dibutyrate binding assay for protein kinase C and related proteins. *Methods Mol. Biol.* **2003**, *233*, 129–156.

(18) Wildman, S. A.; Crippen, G. M. Prediction of physicochemical parameters by atomic contributions. *J. Chem. Inf. Comput. Sci.* **1999**, *39*, 868–873.

(19) Stahelin, R. V.; Digman, M. A.; Medkova, M.; Ananthanarayanan, B.; Melowic, H. R.; Rafter, J. D.; Cho, W. Diacylglycerol-induced membrane targeting and activation of protein kinase Cε. Mechanistic differences between protein kinases Cδ and Cε. *J. Biol. Chem.* **2005**, *280*, 19784–19793.

(20) Garcia-Bermejo, M. L.; Leskow, F. C.; Fujii, T.; Wang, Q.; Blumberg, P. M.; Ohba, M.; Kuroki, T.; Han, K. C.; Lee, J.; Marquez, V. E.; Kazanietz, M. G. Diacylglycerol (DAG)-lactones, a new class of protein kinase C (PKC) agonists, induce apoptosis in LNCaP prostate cancer cells by selective activation of PKC alpha. *J. Biol. Chem.* **2002**, *277*, 645–655 (published erratum appears in **2004**, *279*, 23846.).

(21) Wang, Q. J.; Fang, T. W.; Fenick, D.; Garfield, S.; Bienfait, B.; Marquez, V. E.; Blumberg, P. M. The lipophilicity of phorbol esters as a critical factor in determining the pattern of translocation of protein kinase C delta fused to green fluorescent protein. *J. Biol. Chem.* **2000**, *275*, 12136–12146.

(22) Orynbayeva, Z.; Kolusheva, S.; Livneh, E.; Lichtenshtein, A.; Nathan, I.; Jelinek, R. Visualization of membrane processes in living cells by surface-attached chromatic polymer patches. *Angew Chem., Int. Ed.* **2005**, *44*, 1092–1096.

(23) Katz, M.; Ben-Shlush, I.; Kolusheva, S.; Jelinek, R. Rapid colorimetric screening of drug interaction and penetration through lipid barriers. *Pharm. Res.* **2006**, *23*, 580–588.

(24) Jelinek, R.; Kolusheva, S. Polymerized lipid vesicles as colorimetric biosensors for biotechnological applications. *Adv. Biotech.* **2001**, *19*, 109–118.

(25) Kolusheva, S.; Shalal, T.; Jelinek, R. Peptide−membrane interactions studied by a new phospholipids/polydiacetylene colorimetric vesicle assay. *Biochemistry* **2000**, *29*, 15851–15859.

(26) Takeuchi, K.; Takahashi, H.; Sugai, M.; Iwai, H.; Kohno, T.; Sekimizu, K.; Natori, S.; Shimada, I. Channel-forming membrane permeabilization by an antibacterial protein, sapecin: determination of membrane-buried and oligomerization surfaces by NMR. *J. Biol. Chem.* **2004**, *279*, 4981–4987.

(27) Schwartz, M. A.; Luna, E. J. Binding and assembly of actin filaments by plasma membranes from *Dictyostelium discoideum*. *J. Cell Biol.* **1986**, *102*, 2067–2075.

(28) Blumberg, P. M.; Kedei, N.; Lewin, N. E.; Yang, D.; Czifra, G.; Pu, Y.; Peach, M. L.; Marquez, V. E. Wealth of opportunity: the C1 domain as a target for drug development. *Curr. Drug Targets* **2008**, *9*, 641–651.

(29) Teicher, B. A. Protein kinase C as a therapeutic target. *Clin. Cancer Res.* **2006**, *12*, 5336–5345.

(30) Graff, J. R.; McNulty, A. M.; Hanna, K. R.; Konicek, B. W.; Lynch, R. L.; Bailey, S. N.; Banks, C.; Capen, A.; Goode, R.; Lewis, J. E.; Sams, L.; Huss, K. L.; Campbell, R. M.; Iversen, P. W.; Neubauer, B. L.; Brown, T. J.; Musib, L.; Geeganage, S.; Thornton, D. The protein kinase Cβ-selective inhibitor, enzastaurin (LY317615.HCl), suppresses growth of human colon cancer and glioblastoma xenografts. *Cancer Res.* **2005**, *65*, 7462–7469.

(31) Newman, D. J.; Cragg, G. M. Marine natural products and related compounds in clinical and advanced preclinical trials. *J. Nat. Prod.* **2004**, *67*, 1216–1238.

(32) Hampson, P.; Chahal, H.; Khanim, F.; Hayden, R.; Mulder, A.; Assi, L. K.; Bunce, C. M.; Lord, J. M. PEP005, a selective small-molecule activator of protein kinase C, has potent antileukemic activity mediated via the delta isoform of PKC. *Blood* **2005**, *106*, 1362–1368.

(33) Szallasi, Z.; Smith, C. B.; Pettit, G. R.; Blumberg, P. M. Differential regulation of protein kinase C isozymes by bryostatin 1 and phorbol 12-myristate 13-acetate in NIH 3T3 cells. *J. Biol. Chem.* **1994**, *269*, 2118–2124.

(34) Szallasi, Z.; Denning, M. F.; Smith, C. B.; Dlugoz, A. A.; Yuspa, S. H.; Pettit, G. R.; Blumberg, P. M. Bryostatin 1 protects protein kinase C-delta from down-regulation in mouse keratinocytes in parallel with its inhibition of phorbol ester-induced differentiation. *Mol. Pharmacol.* **1994**, *46*, 840–850.

(35) Patra, S. K. Dissecting lipid raft facilitated cell signaling pathways in cancer. *Biochim. Biophys. Acta* **2008**, *1785*, 182–206.

(36) Stahelin, R. V.; Rafter, J. D.; Das, S.; Cho, W. The molecular basis of differential subcellular localization of C2 domains of protein kinase C-α and group IV acytosolic phospholipase A_2. *J. Biol. Chem.* **2003**, *278*, 12452–12460.

(37) Shaikh, S. R.; Edidin, M. A. Membranes are not just rafts. *Chem. Phys. Lipids* **2006**, *144*, 1–3.

JM900186M